

## Thermal pretreatment of spent button cell batteries (BCBs) for efficient bioleaching

Fatemeh Pourhossein\*, Mohammad Sadeghi\*, and Seyyed Mohammad Mousavi\*<sup>\*,\*\*,\*†</sup>

\*Biotechnology Group, Chemical Engineering Department, Tarbiat Modares University,  
Jalal Ale Ahmad, Nasr, P. O. Box: 14115-111, Tehran, Iran

\*\*Modares Environmental Research Institute, Tarbiat Modares University,  
Jalal Ale Ahmad, Nasr, P. O. Box: 14115-111, Tehran, Iran

(Received 31 January 2022 • Revised 15 April 2022 • Accepted 28 April 2022)

**Abstract**—Spent Zn-Mn button cells are one of the fastest-growing battery waste streams containing considerable amounts of Zn (12-28% (w/w)) and Mn (26-45% (w/w)) that could be considered as a potential industrially demanded source of Mn and Zn. However, due to the very toxic, stable, and refractory nature of the button cell batteries, applying microbial leaching for metal extraction from spent batteries is limited. In this regard, this study focused on detoxicate, enriching, and mobilizing major elements through thermal treatment assisted by acidic bioleaching. It was witnessed after thermal pretreatment of BCBs powder at 600 °C, the *A. ferrooxidans* could tolerate up to 20 g/L BCBs containing a high concentration of Mn and Zn by serial step-wise adaptation process. The use of thermal pretreatment increased by 76% and 75% extraction yields of Mn and Zn compared with the results obtained using un-thermally pretreated BCBs powder. The result indicated that 95% of zinc and 91% manganese were efficiently extracted from thermally pretreated BCBs. *A. ferrooxidans* and Fe<sup>3+</sup> play an important role to improve Mn and Zn extraction efficiency. The structural and morphological analyses showed that the proposed approach could successfully overcome spent button cell batteries complexities and extract most of the major metals.

Keywords: Spent Zn-Mn Batteries, Thermal Pretreatment, Bioleaching, Metal Recovery, *Acidithiobacillus ferrooxidans*

### INTRODUCTION

Button cells as tiny round transportable batteries are widely used in various devices such as hearing aids and wristwatches, thanks to their long operation life, small size, and high energy capacity. Button cells as primary non-rechargeable batteries are divided into different types, such as alkaline, lithium, and silver-oxide, all containing a considerable amount of valuable and heavy metals [1].

Zinc and manganese batteries contain a large percentage of Zn (12-28% (w/w)) and Mn (26-45% (w/w)) can be considered as secondary source of these metals. Mn is the twelfth most abundant element in the Earth's crust, with an average concentration of 1,000 µg/g. Global demand for Mn is projected to reach 28.2 million tons by 2022, while Mn production will fall to 19.1 million tons in the same year. This deep gap between supply and demand for Mn metal will lead to an increase in the price of this metal over the next few years. Therefore, in order to supply Mn in the future, the use of secondary resources must be considered. In fact, spent Zn-Mn batteries can act as artificial mines and Mn can be extracted from them [2].

Heavy metals are dangerous pollutants, as they are not decomposed or perished in the environment [1]. Zn-Mn batteries as alkaline batteries are widely used in different devices. These batteries are estimated to be sold much more extensively than any other type of batteries due to their lower prices. The residue of these batteries

contains Zn, Mn, and Hg, which are highly toxic to humans and the environment if disposed unsafely [3]. Although several legislations prohibit the use of heavy metals in devices and control their dumping, heavy metals are used to some extent in batteries. Furthermore, the production and use of batteries have risen significantly in recent years, causing uncontrolled disposal of batteries. One report shows that almost 88% of dumped button cells were not considered as dangerous wastes and mixed with safe ones [4]. Thus, recycling of these batteries is essential. The disposal of BCBs in landfills results in loss of valuable metals and serious environmental contamination [4,5].

Traditional methods such as hydrometallurgy and pyrometallurgy are being used as recycling methods [6,7]. They use energy and chemical agents to recover heavy metals from wastes, respectively. There have been different studies on the recovery of heavy metals from alkaline batteries through hydrometallurgy process [8-10]. Leaching with sulfuric acid is the most common hydrometallurgical process for recovery of Mn and Zn from alkaline batteries, allowing achieving high zinc dissolution, but manganese recovery is always between 10-43% [11]. Recent publications indicate that manganese recovery from alkaline batteries is always small [12]. Also, acid leaching is expensive and makes secondary pollution in the air and water [3].

Thus, an environmental and effective method of recycling is required for recycling solid wastes [13,14]. Bio-hydrometallurgical process (known as bioleaching) is a growing technology with a remarkable potential that uses bacteria or fungi for metal dissolution from solid waste [15]. Bioleaching is an eco-friendly, cost-efficient, and simple way of recycling in comparison with other conventional methods [16,17]. In general, there are a very limited number of re-

<sup>†</sup>To whom correspondence should be addressed.

E-mail: mousavi\_m@modares.ac.ir

Copyright by The Korean Institute of Chemical Engineers.

ports on the bioleaching of valuable metals from Zn-Mn batteries, and more research is needed on this topic. The bacterial and fungal bioleaching of spent batteries mostly harvests 20-90% of extraction yield for Mn [18,19].

In the spent medium bioleaching method, organic acids produced by *Aspergillus niger* were used to dissolve Ni, Co, Mn, Li, Cu and Al from spent lithium-ion batteries (LIBs) [20]. As reported in our previous study, we have examined the potential for extracting zinc and manganese from spent 'button-cell' batteries by using a culture supernatant of *Acidithiobacillus ferrooxidans* acidophilic bacteria. The maximum recoveries for manganese and zinc were 99% and 53%, respectively, using 10 g/L spent button-cells [21]. The majority of the studies suggest non-contact bioleaching or two-step bioleaching approaches to decrease the negative effect of toxicity of spent batteries on microbial activity. In the current work, we propose the use of thermal pretreatment to improve bioleaching efficiency at high pulp density during one-step bioleaching. In this regard, thermal pretreatment is an interesting option, which has proven to be successful in the minimization of toxicity of the waste at high pulp density in bioleaching process.

There have been different studies using thermal pretreatment in bioleaching as a way to improve the extraction efficiency of heavy metals [22-24]. For example, thermal pretreatment of brake pad waste changed the mode of Cu in the waste from insoluble form to soluble form, which significantly increased the bioleaching of copper [25]. The process of low-temperature treatment is a simple and effective method of removing organic matter and transforming metals to promote bioleaching of heavy metals-containing wastes.

The past works did not consider thermal pretreatment as a means of reducing toxicity of batteries waste for bacteria activity at high content of battery waste. In many cases, manganese was not effectively released from high concentrations of spent Zn-Mn batteries through bioleaching. Up to now, there is no report on using a thermal pretreatment for spent button cell batteries (BCBs) to increase pulp density and manganese recovery in bioleaching process. This study was done to propose a competent and efficient bioleaching process for high extraction of Zn and Mn from spent Zn-Mn button cells at high pulp density. The first aim of the current study is to analyze the reasons for the increase of bioleaching efficiency of Mn and Zn by thermal pretreatment at high pulp density. Accordingly, through this paper, the bioleaching mechanism of thermally treated BCBs was studied in detail to determine reference conditions for bioleaching of Mn and Zn from spent button cell batteries.

## MATERIALS AND METHODS

### 1. Spent BCBs Powder Preparation

Almost 1 kg spent button cells batteries (BCBs) were obtained from various watch stores in Tehran, Iran. BCBs were different in sizes and compositions (based on different manufacturers). Button cells were dismantled manually into different parts, such as anode, cathode caps, plastic separator of anode and cathode, and powder. The powder was dried in an oven at 100 °C (to eliminate the electrolytes) and was then crushed and mixed using a home blender (Moulinex, AR1044, 180 W). It was sieved with a #200 mesh to

obtain a mixed analogous black powder with a particle size of less than 70 µm.

### 2. Characterization of BCBs Powder

The amount of metal content in BCBs was specified after alkaline digestion using an inductively coupled plasma optical emission spectrometer (ICP-OES) (Vista-pro, Varian, Australia). In alkaline digestion, 0.25 g of the un-pretreated and thermal pretreated BCBs powder was placed in a platinum crucible and mixed with sodium-potassium carbonate plus boric acid and heated up to 950 °C in a furnace. The crucible content was cooled and dissolved in HCl (Sigma-Aldrich; ≥99.99%) in ratio of 1 to 1. Then, 5 mL mixture of HNO<sub>3</sub> (Sigma-Aldrich; ≥99.0%) and HCl in a ratio of 1 : 3 was added to the solution and heated for 30 min [26]. After cooling, the solution was filtered and volume was adjusted to 100 mL with distilled water. The concentration of major elements in the solution was determined by inductively coupled plasma optical emission spectrometer (ICP-OES) (Vista-pro, Varian, Australia). The ICP-OES technique extracts elemental information from samples by measuring their emission spectra in order to estimate and identify their concentrations. Plasma is used to desolate, ionize, and excitable excite samples. An element can be identified by its emission lines, and quantified by the intensity of those lines. The wavelengths (nm) used were: Zn: 213.857; Mn: 257.610; Cu: 324.754; Ni: 231.604; Ag: 328.068; Al: 396.152; Pb: 220.353; Cd: 228.802. Before analysis, samples were diluted to reduce matrix interferences. The dilutions performed were 1 : 10 and 1 : 25, depending on the concentration level. The calibration was performed by using a graph of external calibration prepared in the extracting reagent for ICP-OES measurements.

### 3. Thermal Pretreatment of BCBs Powder

Thermal pretreatment was applied on BCBs powder using a thermal gravimetric analyzer-differential thermal analyzer (TGA-DTA; Mettler Toledo, Switzerland) to find the best temperature for thermal pretreatment. TGA analysis is a remarkable method for interpreting the thermal treatment behavior of the powder. It shows the mass loss and rate of mass loss against time and temperature [27]. TG (%) indicates the conventional mass loss of the sample during the pyrolysis process. DTG (%/min) is the mass loss rate of the sample, which is obtained from the first derivative of TG (%) versus time (min). Specifically, 15 mg±1.0 mg powder was placed in Alumina 70 µl sample holder which was used for TGA analysis. Air was used as a carrier gas with a flow rate of 50 mL/min. The sample was heated from room temperature to 1,200 °C with a heating rate of 10 °C/min. To prepare thermally pretreated BCBs powder, BCBs powder was put in a crucible and placed in an electrical furnace (Wisetherm FP, DAIHAN Scientific, South Korea) for 4 h with specific temperature 200 °C and 600 °C based on TGA analysis result.

### 4. Bacteria Inoculum Preparation and Growth Medium

*Acidithiobacillus ferrooxidans* (PTCC 1664) as an iron-oxidizing bacterium was used for bioleaching the spent BCBs powder. It was purchased from Iranian Research Organization for Science and Technology (IROST), Tehran, Iran. The medium used for this bacteria was 9 K, which contains 44.48 g FeSO<sub>4</sub>·7H<sub>2</sub>O (Sigma-Aldrich; ≥99.5%), 3.00 g (NH<sub>4</sub>)<sub>2</sub>SO<sub>4</sub> (Sigma-Aldrich; ≥99.0%), 0.1 g KCl (Sigma-Aldrich; ≥99.0-100%), 0.50 g MgSO<sub>4</sub>·7H<sub>2</sub>O (Sigma-Aldrich; ≥99.5%), and 0.01 g Ca(NO<sub>3</sub>)<sub>2</sub> (Sigma-Aldrich; ≥99.0%) [28] in

1,000 mL deionized water. The pH of the medium for the growth of the bacteria was adjusted to 2 by sulfuric acid 98% solution. Growth curves of bacteria were obtained by directly contacting them in liquid solution. Samples for bacterial counting were put on a Neubauer chamber (with a depth of 0.1 mm and an area of 0.0025 mm<sup>2</sup>) under a phase-contrast microscope (ABS 120-4 Zeiss, Germany) with 400X magnification. Using the number of cells in the chamber, the concentration or density of the cells in the mixture that contains the sample can be calculated. Counting cells in a high cell concentration requires diluting the suspension to a level low enough for the density to be low enough. In that case, the final count must be multiplied by the dilution factor.

### 5. *A. ferrooxidans* Adaptation Process

Adaptation of bacteria was done via serial sub-culturing method for both pretreated and un-pretreated BCBs powders [29]. First, adaptation was started with 0.1% (w/v) of pretreated and un-pretreated BCBs powder in a 250 mL Erlenmeyer flask containing 9K medium with 10% (v/v) active *A. ferrooxidans* culture with a cell density of  $>1 \times 10^7$  cells/mL. The adaptation process was performed in eight steps: 1, 2.5, 5, 7.5, 10, 15, 20 and 25 (g/L) BCBs-600 °C. In each step, when the bacterial cell density reached  $5 \times 10^7$  cell/mL, the flasks were put aside for 1 h to separate adapted bacteria cells from BCBs-600 °C powder and used as inoculum for the next step with more concentration of BCBs-600 °C powder. At the end of the adaptation process, the flask containing a high concentration of BCBs-600 °C was centrifuged for separating the adapted free bacteria cells from solid powder. Then, 10 mL of supernatant was added to 90 mL of 9K media for preparing a pure culture of adapted *A. ferrooxidans* for all bioleaching experiments. All flasks were placed in a shaker incubator (WIS-20R WiseCube, South Korea) at 140 rpm and 30 °C for 21 days.

### 6. Bioleaching Experiments

Two different bioleaching methods based on the presence of bacteria were used for zinc and manganese extraction from BCBs-600 °C powder.

#### 6-1. One-step Bioleaching

In the one-step bioleaching method, 2% (w/v) of BCBs-600 °C powder was added to 90 mL 9K medium, after which the pH of the medium was adjusted to 2.0 by 98% sulfuric acid [30]. Next, inoculation was performed by adding 10% (v/v) adapted *A. ferrooxidans*. The flask was placed in a shaker incubator at 140 rpm and 30 °C for 21 days.

#### 6-2. Spent Medium Bioleaching

In the spent medium bioleaching method, first 10% (v/v) of adapted *A. ferrooxidans* was added to 9K medium and cultured until logarithmic phase (5<sup>th</sup> day) when the ferric ion concentration as the main metabolite produced by *A. ferrooxidans* reached 6 g/L. Biogenic metabolites generated by bacteria were separated from *A. ferrooxidans* cells through centrifugation at 12,000 g for 15 min at 4 °C. Then, 20 g/L BCBs-600 °C powder was added to bio-metabolite and was placed in a rotary shaker with 140 rpm and 30 °C for 21 days [31].

During the bioleaching process, every two days, biochemical parameters including pH, Eh, Fe<sup>3+</sup> concentration, and cell density were measured to have a better understanding of bioleaching procedure. To determine the concentration of metals in the bioleach-

ing solution over time, 5 mL of bioleaching solution sample was taken from each flask and centrifuged at 3,000 g for 2 min and passed throughout Millipore filter to remove solid particle for ICP-MS (Vistapro, Varian, Australia) analysis. All experiments were run in triplicate with mean values considered. During the bioleaching period, water evaporation was compensated with injecting distilled water in to all flasks.

### 7. Leaching by Chemical Ferric

Ferric iron is the main metabolite generated by *A. ferrooxidans* in the logarithmic phase through ferrous sulfate oxidation. To investigate the role of biological ferric ion in metal extraction during bioleaching of metals from BCBs-600 °C, leaching through chemical ferric sulfate (Fe<sub>2</sub>(SO<sub>4</sub>)<sub>3</sub>) (Sigma-Aldrich;  $\geq 99.5\%$ ) was done. In leaching by chemical ferric sulfate experiment, 24.39 g Fe<sub>2</sub>(SO<sub>4</sub>)<sub>3</sub> (6.83 g/L ferric ion) was added to 1,000 mL of distilled water and mixed for 1 h. 20 g/L BCBs-600 °C powder was added to a aforementioned solution [32]. The flask was put in a shaker incubator at 140 rpm and 30 °C for 21 days. At the end of this period, samples were taken for ICP-MS analysis to examine the extraction of selected metals, and further compared with metal recovery efficiency via the bioleaching process.

### 8. Analytical Procedure

pH variation of each flask was measured by a digital pH meter (CP-500L, ISTEK, South Korea) during bioleaching. The oxidation and reduction changes were also monitored by an Eh meter (691 Metrohm, Switzerland). Ferric ion concentration was measured by 5-Sulfosalicylic acid (SSA) colorimetric method [33]. The standard line was prepared by chemical ferric sulfate in distilled water within the range of 1 to 10 g/L with absorbance measured at 500 nm.

Different analyses including XRD (X'Pert MPD, Philips, Netherlands) and SEM-EDX (CamScan MV2300, Czech Republic) were performed on thermally pretreated and un-pretreated BCBs powder before bioleaching to indicate the effect of thermal pretreatment and bioleaching BCBs powder structure.

## RESULTS AND DISCUSSION

### 1. Thermal Pretreatment

#### 1-1. TGA Analysis of BCBs Powder

Fig. 1 displays the thermal behavior of BCBs powder under TGA analysis. As can be seen, the percentage of weight loss was measured within 200-1,200 °C. The thermal treatment process of BCBs powder could be divided into three stages. It was shown that the powder has a greater reaction within this range of temperature where decomposition and weight loss occur faster. The first weight loss of around 1% was observed between 25 °C and 100 °C, which is attributed to evaporation of physically absorbed water in the powder [34]. The second loss of weight of about 3% from 236 °C to 330 °C, with a sharp peak at 200 °C probably due to C was burnt [35]. The weight-loss region is between 250 °C and 600 °C, which is ascribed to the complete ignition of organic matters (acetylene black and PVdF) in the powder and decomposition of ZnMn<sub>2</sub>O<sub>4</sub> and ZnO causing almost 13% weight loss [36]. It is noteworthy that ZnO that exist in BCBs powder can be reduced to metallic zinc according to the following reactions [22,37]:

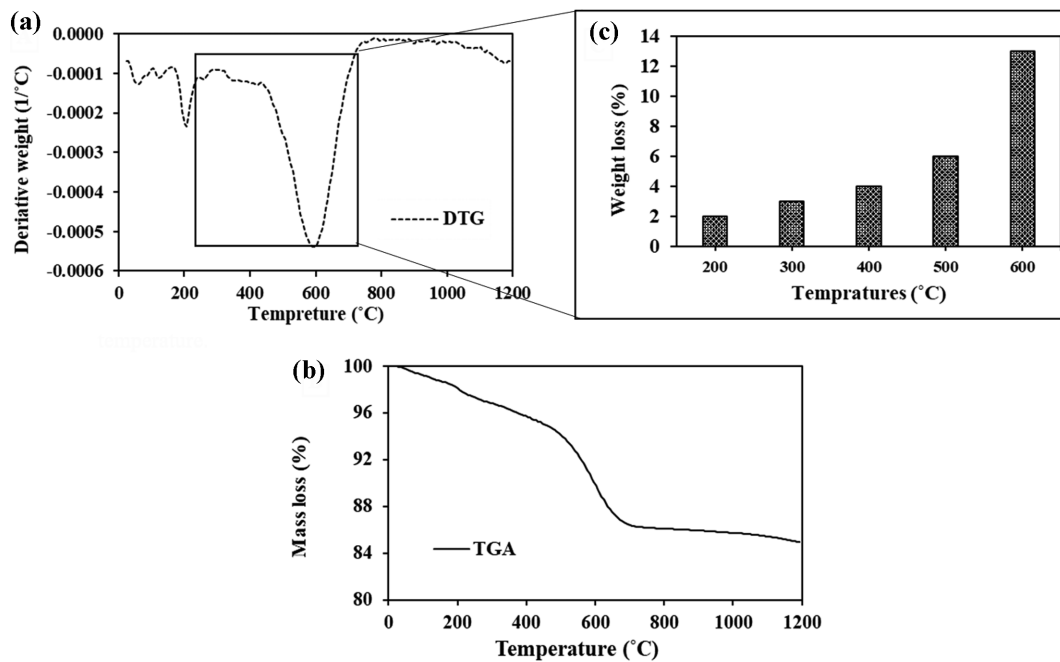


Fig. 1. (a) Derivative Thermogravimetry; (b) thermogravimetric analysis of BCBs powder, (c) the mass loss during 200-600 °C.



Eq. (1) occurs in an inert atmosphere, which means that carbon is needed for the reduction of ZnO. Carbon can be provided from the graphite of batteries. To avoid the simultaneous reaction of the carbon with the oxygen of air, the reaction has to be carried out in inert atmosphere. On the other hand, Eq. (2) occurs in the presence of air or CO<sub>2</sub>. At high temperatures, oxygen reacts with carbon and produces carbon dioxide (Eq. (3)), which reacts with carbon and produces carbon monoxide (CO<sub>2</sub>+C→2CO) that reduces the zinc present in the zinc-bearing phases to metallic zinc [38]. Also, there is a small loss of weight between 600 °C and 1,200 °C that is due to the complete combustion of organic matter in BCBs powder. A total weight loss of 16% was observed in the entire range of temperature that was attributed to the evaporation of oxygen from the BCBs powder. Based on the weight loss rate graph of BCBs original powder, two temperatures of 200 °C and 600 °C were chosen for thermal pretreatment as the best calcination temperature.

#### 1-2. BCBs Powder Composition

Table 1 reports the ICP-MS results of digested BCBs powders before and after thermal pretreatment at two temperatures. The original BCBs powder contains approximately 26.5% Mn, 16.5% Zn, 4.9% K, and a low concentration of Ni, Ca, Cu, Cr, Al, and Mg (≤0.02%). The carbon content was approximately 9.37% (w/w). After thermal pretreatment at 200 °C and 600 °C, 0.52 g and 2.18 g total mass of BCBs powder decreased. The metal concentrations increased to 54% (w/w) and 56% (w/w), at 200 °C and 600 °C, respectively. The metals Zn and Mn were identified as major elements in un-pretreated BCBs powder with 26.5% and 16.5% (w/w).

Table 1. The metal content of BCBs powders before and after thermal pretreatment

Metals	Original BCBs (%w/w)	BCBs-200 °C (%w/w)	BCBs-600 °C (%w/w)
Mn	26.5	28.7	29.2
Zn	16.5	18.46	19.21
K	4.9	5.3	5.7
Cd	0.68	0.72	0.78
Ag	0.42	0.48	0.5
Na	0.26	0.29	0.35
Cu	0.1	0.15	0.21
Fe	0.09	0.1	0.12
Ni	0.19	0.08	0.1
Ca	0.03	0.03	0.03
Al	0.02	0.01	0.02
Mg	0.02	0.02	0.02

It can be seen that Mn and Zn weight percentage rose to 29% and 19% (w/w) through raising the thermal pretreatment temperature from 200 °C to 600 °C due to the combustion of the volatile fraction of the BCBs powder such as black carbon. Also, the changes in the color of BCBs powder from black to dark brown at 600 °C were probably cleared that the carbon in the spent Zn-Mn battery was totally burned out at temperatures above 200 °C.

#### 1-3. XRD, SEM and Mapping Analysis of BCBs Before and After Thermal Pretreatment

XRD analysis was employed to investigate the changes in the mineralogy of samples before and after thermal pretreatment at 200 °C and 600 °C based on TGA analysis (Fig. 1). According to the results (Fig. 2), the original spent BCBs powder contained dif-

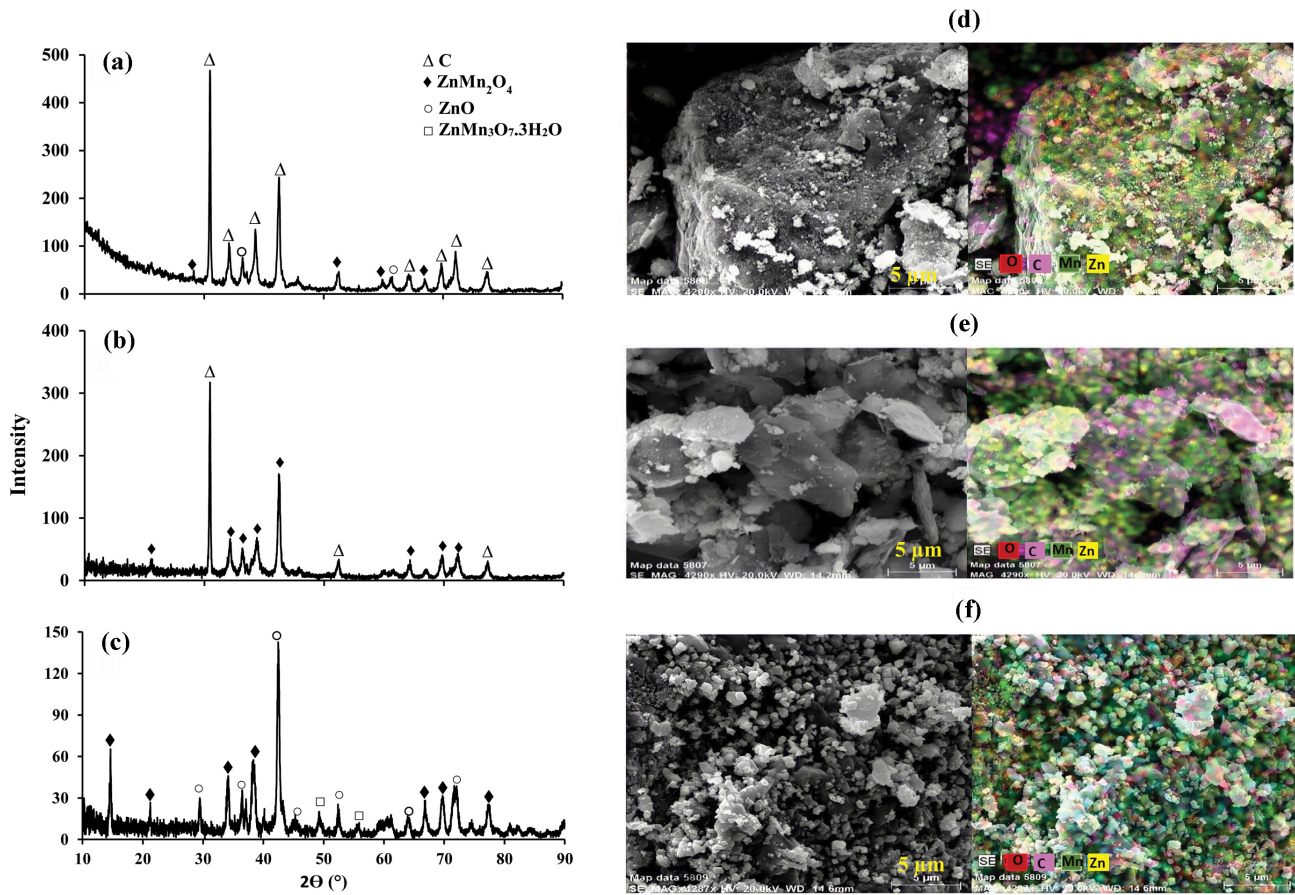


Fig. 2. XRD pattern of (a) original BCBs; (b) BCBs-200 °C; (c) BCBs-600 °C; SEM-Mapping images of (d) original BCBs; (e) BCBs-200 °C; (f) BCBs-600 °C.

ferent main phases of graphite (C), zinc oxide (ZnO), and hetaerolite ( $\text{ZnMn}_2\text{O}_4$ ) [39,40], where a large amount of non-metal compound complicates the efficient release of metals during bioleaching process. After thermal pretreatment, the diffraction peak of carbon totally disappeared with an increase in temperature. The absence of a carbon peak confirms its conversion to carbon dioxide (Eq. (3)) [24]. At 200 °C, the phase composition of the BCB powder was not changed, while the low temperature thermal pretreatment might cause quantitative changes in the phase compositions [24].

At 600 °C, the phase composition of the thermally pretreated sample changed, and the main phases identified in this sample ( $\text{ZnMn}_2\text{O}_4$ ,  $\text{ZnMn}_3\text{O}_7$ , ZnO) are shown in Fig. 2(c). The characteristic peaks suggest that  $\text{ZnMn}_2\text{O}_4$  structure will decompose to ZnO and  $\text{ZnMn}_3\text{O}_7 \cdot 3\text{H}_2\text{O}$  (soluble form) by increasing thermal pretreatment from 200 °C to 600 °C. As mentioned, at higher temperatures, the C decomposition leads to a reduction process for ZnO [22]. Therefore, this reduction led to more reachability of Zn in bioleaching process.

The effect of thermal pretreatment on the surface morphology of the original BCBs powder was observed via SEM and mapping analysis, Fig. 2. As shown, unpretreated BCBs powder has a smooth surface without any significant pores (Fig. 2(d)). The SEM pictures of the pretreated powders at 200 °C and 600 °C (Fig. 2(d) and (f)) show microstructural changes in the surface of BCBs powder due

to thermal pretreatment. The thermal pretreatment has a significant effect on BCBs powder surface structure and particle size. The roughness and porosity of the surface of the original BCBs powder increased by raising the thermal pretreatment temperature from 200 °C to 600 °C. The 600 °C-thermal treatment altered the morphology and components of BCBs more than the 200 °C-heat treatment. A more needle-like or rod-like matter representing Mn/Zn oxides appears in the surface of BCBs powder when organic matter surrounding the batteries has been removed. Therefore, more reactive and fresh surfaces will be accessible for microorganisms and lead to better metal mobilization during the bioleaching process. Fig. 2(f) depicts that the particle size of BCBs powder diminished after thermal pretreatment at 600 °C. The mapping analysis shows that by increasing the pretreatment temperature from 200 °C to 600 °C, the carbon content significantly decreased, while the amount of Mn and Zn increased as shown clearly by the color green and yellow.

## 2. Effect of Thermal Pretreatment on the Extraction of Zn and Mn from BCBs Powder

Based on Fig. 3, *A. ferrooxidans* cannot grow in the presence of un-pretreated BCBs powder and pretreated BCBs powder at 200 °C, but they could grow in the presence of pretreated BCBs powder at 600 °C. The effect of thermal pretreatment on bacterial growth and activity was investigated at 1 g/L of un-pretreated, pretreated-

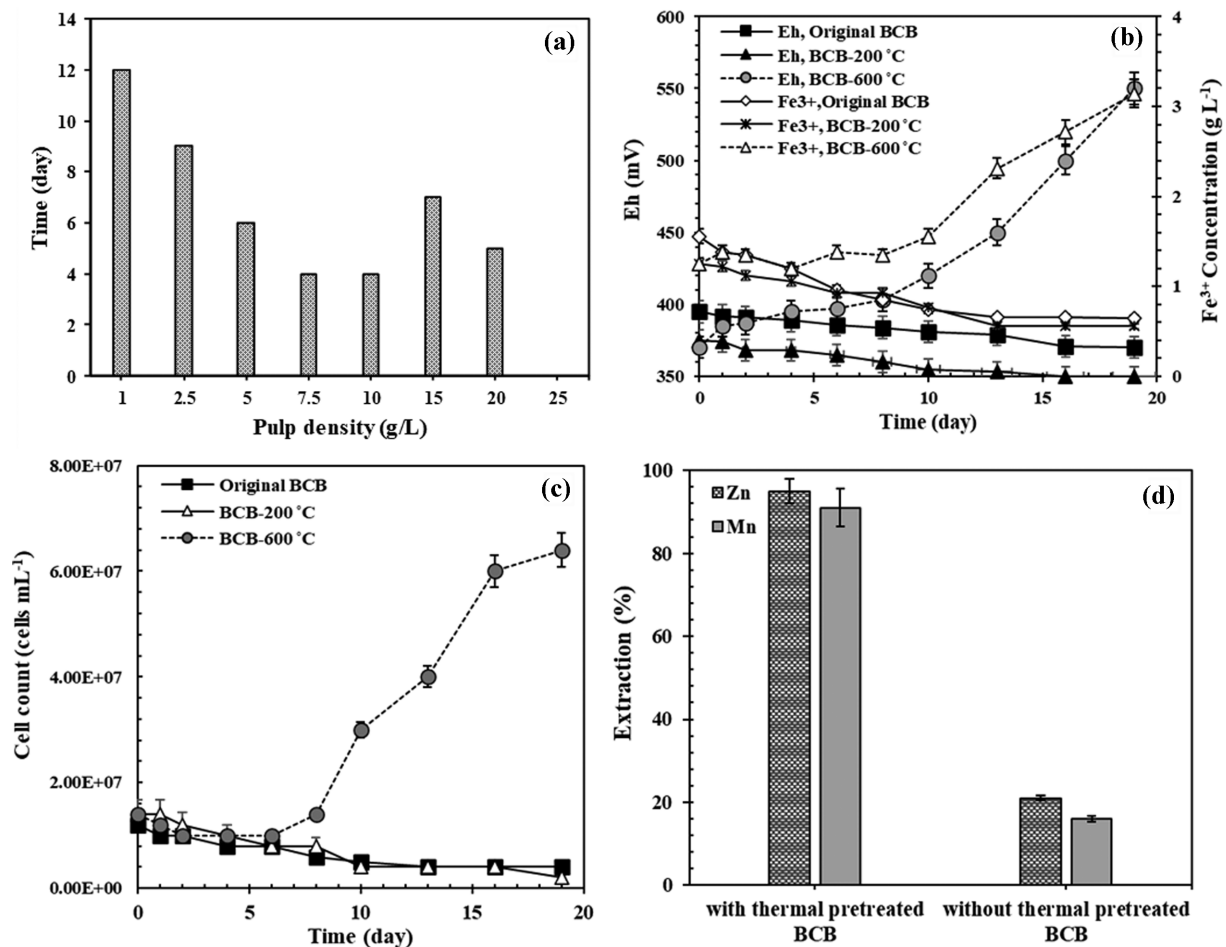
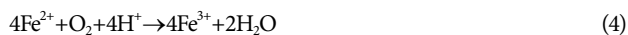


Fig. 3. (a) The time needed during the adaptation of *A. ferrooxidans* to BCBs-600 °C; the variations in (b) Eh and Fe<sup>3+</sup> ion concentration; (c) cell count in presence of 1 g/L BCBs, BCBs-200 °C and BCBs-600 °C; (d) metals extraction efficiency with 20 g/L original BCBs and BCBs-600 °C.

200 °C, and pretreated-600 °C BCBs powder (Fig. 3(b)-(c)). As compared to *A. ferrooxidans* ability in presence of un-pretreated BCBs and BCBs-200 °C, *A. ferrooxidans* has more tolerance for BCBs-600 °C. The results related to the ferric concentration and oxidation-reduction potential indicated that *A. ferrooxidans* cell does not have any activity in the presence of unpretreated BCBs and BCBs-200 °C powder; it was most probably because of the hazardous nature of carbon in unpretreated BCBs for bacterial growth and activity [41,42]. After thermal pretreatment at a suitable temperature (600 °C), carbon completely is removed in BCBs powder and also changes the powder structure and composition to a soluble form. Thus, *A. ferrooxidans* could grow after a long lag phase (12 days). Metabolic processes such as ferrous sulfate bio-oxidation in *A. ferrooxidans* cause the production of main metabolites such as ferrous sulfate and protons (Eqs. (4)-(7)) [43]. The production of these metabolites increases Eh values. A sharp increase in Eh means the bacteria entrance into the logarithmic phase [44].



To achieve a high concentration of BCBs powder, the adaptation process of *A. ferrooxidans* was done from 1 g/L to 25 g/L BCBs-600 °C powder using serial subculture method [45]. The time required for the adaptation of *A. ferrooxidans* to BCBs-600 °C is shown in Fig. 3(a). The longest required time (12 days) for bacterial adaptation was at 1 g/L with the adaptation time decreasing by increasing the solid concentration until 10 g/L. This is because *A. ferrooxidans* cells under stress change the synthesis of particular proteins, making the bacteria immune to a toxic environment where the bacterial tolerance to the high concentration of heavy metals grows constantly [46]. In the presence of 20 g/L BCBs-600 °C, the adaptation time decreased to five days since the biochemical resistance mechanism of bacteria against heavy metals improved during the adaptation process. The highest solid concentration tolerable by bacteria was 20 g/L beyond which (25 g/L), *A. ferrooxidans* could not grow. This is because, the toxic metal concentration of BCBs-600 °C powder was more than the bacteria tolerance level and the high concentration of heavy metals harming the bacteria cell membrane [47]. So, it is reasonable to conclude that the perfect cooperation between thermal pretreatment at a suitable temperature and

adaptation process is absolutely promising to achieve a strain with resistance to a high concentration of BCBs powder.

The effect of thermal pretreatment on Zn and Mn bioleaching was studied using unpretreated BCBs and BCBs-600 °C samples. According to Fig. 3(d), in comparison to bioleaching with unpretreated BCBs, bioleaching with BCBs-600 °C exhibited good performance on the extraction of metals from BCBs powder. The Zn and Mn extraction efficiency through bioleaching with unpretreated BCBs powder was 21% and 16%, respectively. The waste contains various components, causing a negative effect on bacterial growth during the bioleaching process. The lack of bacterial activity in presence of unpretreated BCBs led to low leaching yields of metals. In bioleaching with unpretreated BCBs powder, the results show that the abiotic H<sub>2</sub>SO<sub>4</sub> has a slight effect on the bioleaching of Zn and Mn through a chemical reaction. The main reason for the low recovery rate of Mn, and Zn was insoluble Mn and Zn in spent BCB matrix in a high percentage, which brought about the toxic and alkaline medium for acidophilic bacteria and decreased the activity. The result suggested that for the conversion of insoluble MnO<sub>2</sub> to Mn<sup>2+</sup>, a strong reducing agent, namely ferrous ion, is vital. In bioleaching with thermally pretreated BCBs powder, the reaction between H<sup>+</sup> and Fe<sup>3+</sup> as leaching agents with a metal component results in high extraction of metals from BCBs powder [39, 44,48]. Here, thermal pretreatment improved the bioleaching performance by changing the refractory form of Zn and Mn into a tractable form [25]. After thermal pretreatment, ZnMn<sub>3</sub>O<sub>7</sub> was formed and the leachability of Mn was improved. The strong transformation of Mn/Zn oxides resulted in a large amount of trackable ZnO and ZnMn<sub>2</sub>O<sub>4</sub>, which could be effectively extracted by autotrophic bioleaching for the maximum mobilization of both Mn and Zn [49]. ZnMn<sub>2</sub>O<sub>4</sub> is composed of soluble ZnO, MnO and insoluble MnO<sub>2</sub>. Mn and Zn in ZnO and MnO are easily released via acidolysis by biogenic H<sup>+</sup>, and Mn<sup>4+</sup> in MnO<sub>2</sub> is extracted through reduction by bio-derived Fe<sup>2+</sup> and acidolysis by biogenic H<sup>+</sup> [3,12,21]. As a result of the 600 °C thermal treatment, the refractory Mn/Zn carbonates are transformed into trackable MnO and ZnO, and the carbon organic matter surrounding the BCB is removed, facilitating acidolysis and reduction reactions. The 600 °C-heat treatment enhanced the formation of ZnMn<sub>2</sub>O<sub>4</sub> and ZnO due to stronger oxidation at higher temperatures, which positivity affected the bioleaching capability of Mn and Zn. Accordingly, the highest temperature of 600 °C caused the BCB structure to collapse, leading to a rapid and successful bioleaching of both Mn and Zn from the BCB at 600 °C.

Additionally, siderophores are organic ligands in a large number of bacteria and fungi in iron deficiency conditions. Most siderophores have several functional groups, such as hydroxamates, catecholamines, and carboxylates for metal bonding. Siderophores can solubilize Mn; the Mn-siderophores can reduce the toxicity of this metal for microorganisms when there is a high concentration of this metal [50].

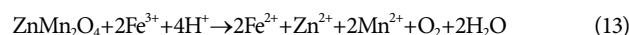
As can be seen in SEM images, the particle size of BCBs powder decreased after thermal pretreatment where generally small particles facilitate Mn and Zn extraction because of increased mass transfer [42]. Thermal pretreatment increases the active surface area by decreasing the BCBs particle size for leaching agent pene-

tration into the particle. Also, the thermal pretreatment causes erosion on the original BCBs sample surface, thus increasing porosity and surface roughness. The surface roughness and smaller particle size must be taken into consideration for a successful bioleaching process.

### 3. Extraction of Zn and Mn from Thermal Pretreated BCBs by Different Methods

According to Fig. 4, in comparison to chemical leaching and spent medium bioleaching, one step bioleaching exhibited a good performance on the extraction of metals from BCBs powder. At 20 g/L of BCBs-600 °C, 95% of Zn and 91% of Mn were extracted in 21 days by one-step bioleaching process. The oxides ZnMn<sub>2</sub>O<sub>4</sub>, ZnMn<sub>3</sub>O<sub>7</sub>, ZnO were observed in the samples after thermal pretreatment at 600 °C. Under acidic conditions, ZnMn<sub>2</sub>O<sub>4</sub> and ZnMn<sub>3</sub>O<sub>7</sub> decompose and ZnO, MnO, and MnO<sub>2</sub> are released in the solution (Eq. (8)-(9)). As mentioned, in the bioleaching process, there are two intermediate metabolites, (H<sup>+</sup>) and (Fe<sup>3+</sup>), used for metal extraction [51]. Fe<sup>3+</sup> as an oxidizing agent attacked the BCBs-600 °C matrix, reacted with Zn and Mn compounds, and were converted to Fe<sup>2+</sup> ions. Then Fe<sup>2+</sup> ions were oxidized to Fe<sup>3+</sup> by the bacteria for gaining energy. Zn and Mn solubilization occur through a cycle between Fe<sup>2+</sup> and Fe<sup>3+</sup>. Furthermore, the reaction of Zn and Mn extraction from BCBs-600 °C powder occurred through reduction of ZnO, MnO, and MnO<sub>2</sub> via H<sup>+</sup> produced by bacteria in bioleaching solution (Eq. (10)-(14)) [52,53]. The oxygen atoms in this metal-oxide are attacked by H<sup>+</sup>, and the protonated atoms of oxygen hydrolyzed and the metals (Zn and Mn) detached from the BCBs-600 °C matrix.

In the BCBs-600 °C powder, Mn is present in different forms (Mn<sup>2+</sup>, Mn<sup>4+</sup>) [12,54]. The Eh-pH diagram of the Mn-H<sub>2</sub>O and Zn-H<sub>2</sub>O systems indicated that Mn<sup>2+</sup> and Zn<sup>2+</sup> can be dissolved in the acidic region. But Mn<sup>4+</sup> will need a strong acidic condition to form Mn<sup>2+</sup> [36]. Fig. 4(b) and (c) display pH and Eh variations during bioleaching of BCBs-600 °C powder. The rise in the pH of the sample in the first days of one-step bioleaching is owing to the alkaline nature of the BCBs. This means that the H<sup>+</sup> produced by the bacteria (according to Eqs. (5)-(7)) were consumed by acid-consuming components; thus, the metals present in the BCBs-600 °C powder were released. Also, an increase in pH can be attributed to the oxidation of Fe<sup>2+</sup> to Fe<sup>3+</sup>. ZnO and MnO present in BCBs-600 °C powder rapidly used the H<sup>+</sup> of the medium and increased the pH of the bioleaching solution (Eq. (8)-(10)). Note that for conversion of insoluble Mn<sup>4+</sup> to soluble Mn<sup>2+</sup>, a strong reducing agent namely Fe<sup>2+</sup> is required (Eq. (14)) [55]. On the other hand, the Fe<sup>3+</sup> from oxidation of Fe<sup>2+</sup> in Eq. (14) caused a series of chemical reactions to produce Fe<sup>2+</sup>. Metals solubilization can occur through this cycle between Fe<sup>2+</sup>/Fe<sup>3+</sup> [56].



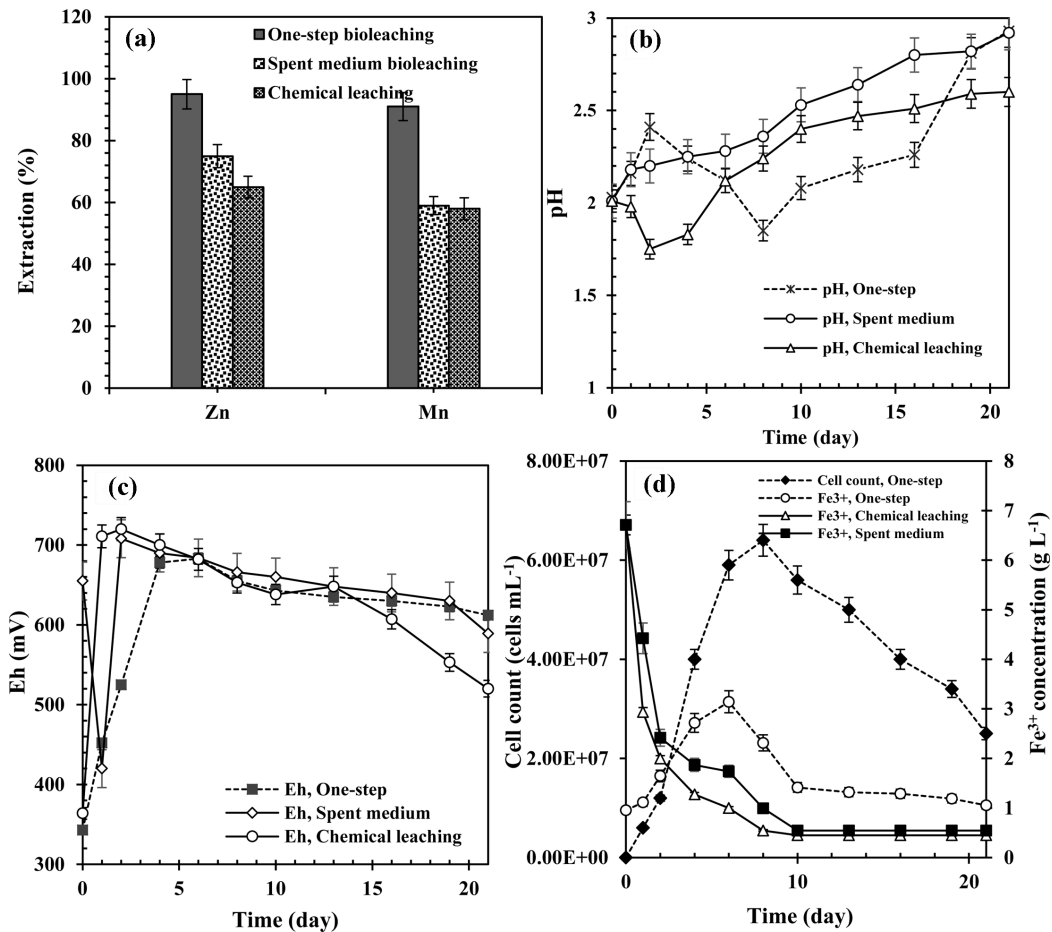
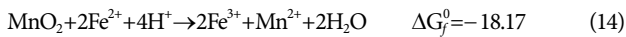


Fig. 4. (a) Metals leaching efficiency, changes (b) pH; (c) Eh; (d) cell count and  $\text{Fe}^{3+}$  over time by different bioleaching and leaching methods.



The extraction yields of Zn and Mn through the bioleaching by spent medium are less than the values of one-step bioleaching at the same time. This can be related to the lack of bacterial activity in spent medium bioleaching. Since spent medium bioleaching, bacteria separated from bio-metabolite, so  $\text{Fe}^{3+}$  and  $\text{H}^+$  cannot be reproduced as a reagent for extraction of metals. Thus, during one-step bioleaching, there is a far greater leaching agent to dissolve both Zn and Mn than spent medium bioleaching. Therefore, *A. ferrooxidans* and  $\text{Fe}^{3+}$  play an important role; in this process the bacteria accelerated the proton and electron transfer.

Mn reducing microorganisms require direct contact with the residue to reduce manganese. There is the Mn reductase enzyme in the cell membrane of microorganisms. Mn plays an important role as a catalyst and cofactor in the microorganism and also participates in several reduction-oxidation processes.  $\text{MnO}_2$  was used in direct contact with microorganisms instead of oxygen as the final receptor for electrons in the respiratory chain (Eq. (15)).



On other hand, in one-step bioleaching process, the presence of the EPS layer on the cell surface is an important factor in the attachment of bacteria to solid surfaces [57,58]. The EPS causes the ad-

hesion of the cells to sample and the highly concentrated  $\text{Fe}^{2+}/\text{Fe}^{3+}$  cycle causes the reduction of insoluble Mn. Also, EPS can help to dissolve insoluble metals [59,60]. For better understanding, there are many OH and COOH groups in EPS so that when these compounds react with  $\text{Fe}^{3+}$  which release  $\text{H}^+$  into the environment and the acidity of the environment increases according to Eq. (16) [33]



In the spent medium bioleaching and chemical leaching, there are no bacteria for the reproduction of  $\text{H}^+$  and  $\text{Fe}^{3+}$ , so the pH of bioleaching solution increased constantly over time. At the beginning of the spent medium bioleaching process, the Eh of the bioleaching solution decreased to 450 mV and  $\text{Fe}^{3+}$  concentration dropped from 6.7 g/L to less than 4 g/L. It can be attributed to two reasons: (1) ferric ion attacks the metallic elements and metals mobilized into the bioleaching solution (Eqs. (13)); and (2)  $\text{Fe}^{3+}$  makes a complex with the medium component (Eq. (17)) and forms jarosite, which is an insoluble component. Note that the jarosite formation reaction during bioleaching process usually happens at higher pH values ( $\geq 2.2$ ) [61,62]. According to Fig. 4(c) after two days, the Eh of the leach suspension rapidly increased, which is related to the reaction between ferric ion and  $\text{ZnMn}_2\text{O}_4$  oxygen produced [63]. In the one-step bioleaching, the presence of bacteria led to the consumption of oxygen and the value of Eh is lower than spent

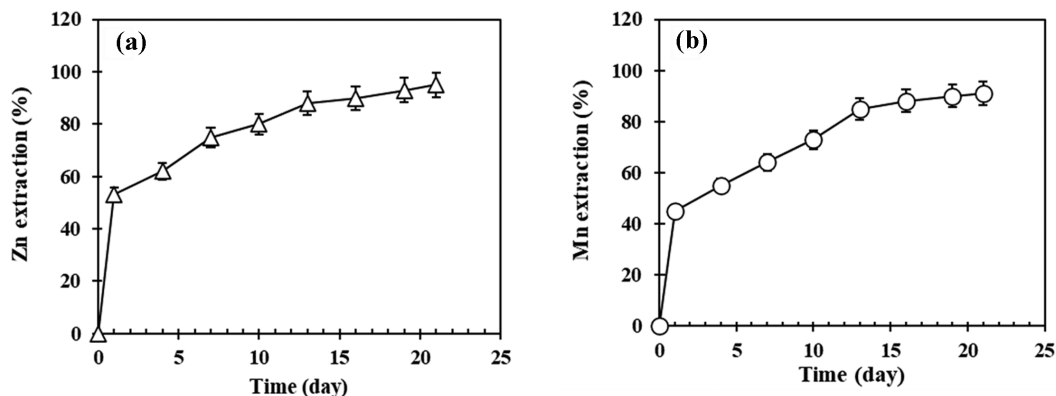


Fig. 5. Extraction of (a) Zn and (b) Mn over time in one-step bioleaching.

medium bioleaching.



The Zn and Mn extraction efficiency through leaching by chemical ferric was 65% and 55%, respectively. In bioleaching, metal leach yields were greater than those obtained through chemical leaching, demonstrating the advantage of bioleaching in metal extraction from BCBs. In the one-step bioleaching, the  $\text{Fe}^{3+}$  and  $\text{H}^+$  were constantly generated in a green way by a series of biochemical reactions (Eq. (2)). Also, the better performance of bioleaching is related to other metabolites such as amino acids and organic compounds, which may be produced by bacteria during the bioleaching process [32].

As can be seen in Fig. 5(a) and (b), more than 50% of the recover for Zn and Mn occurred on the first day of bioleaching due to the high concentration of the leaching agent ( $\text{H}^+$ ). In the following days, the  $\text{Fe}^{3+}$  concentration increased with the growth of the bacteria (Fig. 4(c)) while pH dropped slightly. The increase in  $\text{Fe}^{3+}$  concentration led to enhanced metal recovery over time. Fig. 5 indicates that on early days, zinc and Mn were dissolved by  $\text{H}^+$  as a leaching agent, and then the metals were leached by the produced  $\text{Fe}^{3+}$ . After 10 days, The  $\text{Fe}^{3+}$  concentration decreased from 7 g/L to 1 g/L at metal leach yields increased and reached the highest metal extraction efficiency at the end of the 21<sup>st</sup> day. Also, the reduction in  $\text{Fe}^{3+}$  concentration can be related to the formation of the jarosite passive layer (Eq. (17)) on the BCBs-600 °C powder surface [64]. There is no significant increase in metal leach yields after 15 days, which may be due to the jarosite layer covered BCBs-600 °C surface inhibiting the diffusion of leaching agent to the inside of solid powder.

#### 4. Bioleaching Mechanism Exploration of the BCBs Battery Powder by SEM-EDX and XRD Analysis

The effect of the bioleaching process on BCBs-600 °C powder was characterized by structural analysis by SEM-EDX and XRD after one-step bioleaching. The surface of the BCBs-600 °C powder before bioleaching is non-porous and it turns into a porous surface in response to bioleaching (Fig. 6(a)). Also, the cubic structure on the surface of bioleached BCBs-600 °C powder is related to K-jarosite [61].

Fig. 6(b) reveals the mapping images of BCBs-600 °C after bio-

leaching. Most of Mn and Zn was dissolved by a one-step bioleaching process. The results of EDX analysis of BCBs-600 °C after bioleaching are shown in Fig. 6(c) and (d). Also, the amount of Zn and Mn significantly diminished after one-step bioleaching, suggesting the high extraction efficiency of Zn and Mn from BCBs powder. Finally, the EDX analysis of bioleached BCBs indicated jarosite layer formation on BCBs powder surface. The XRD pattern of the bioleached BCBs-600 °C (Fig. 6(e)) shows that sharp peaks could be attributed to K-jarosite, formed as the passivation layer on the BCBs-600 °C surface during one-step bioleaching by *A. ferrooxidans* and due to inhibition of complete metal dissolution [65]. Also, according to characteristic peaks after bioleaching, the peaks related to ZnO and  $\text{ZnMn}_2\text{O}_7$  completely disappeared and peaks related to  $\text{ZnMn}_2\text{O}_4$  significantly decreased, because of high Mn and Zn extraction during the one-step bioleaching process. The  $\text{ZnMn}_2\text{O}_4$  was still identified in the bioleached residue, indicating that bioleaching is ineffective for this solid phase.

#### CONCLUSION

The present work studied the enhancement of Zn and Mn bioleaching from spent button cell batteries via a temperature thermal pretreatment. In the first step (thermal treatment), the thermal analysis of the waste powder indicated that the suitable temperature for thermal treatment of spent BCBs is 600 °C. Characterization of thermal treated spent BCBs (BCBs-200 °C, BCBs-600 °C) in terms of its structural and morphological using different analyses indicated how the thermal treatment affects and promotes the waste properties. In the second step (acidic bioleaching), the thermal treatment affects the bacterial performance in the bioleaching process by detoxicating and change of the spent BCBs powder composition from a very stable and insoluble to a soluble form. After thermal pretreatment, the *A. ferrooxidans* could tolerate up to 20 g/L spent BCBs containing high concentrations of Mn and Zn by serial adaptation process. Under thermal pretreatment, the acid-insoluble  $\text{ZnMn}_2\text{O}_4$  changes into an acid-soluble form, thereby promoting the bioleaching performance of Mn and Zn. Also, it was found that the extraction yields of Zn and Mn through the bioleaching by spent medium are less than the values of one-step bioleaching at the same time. At 20 g/L BCBs-600 °C, bioleaching

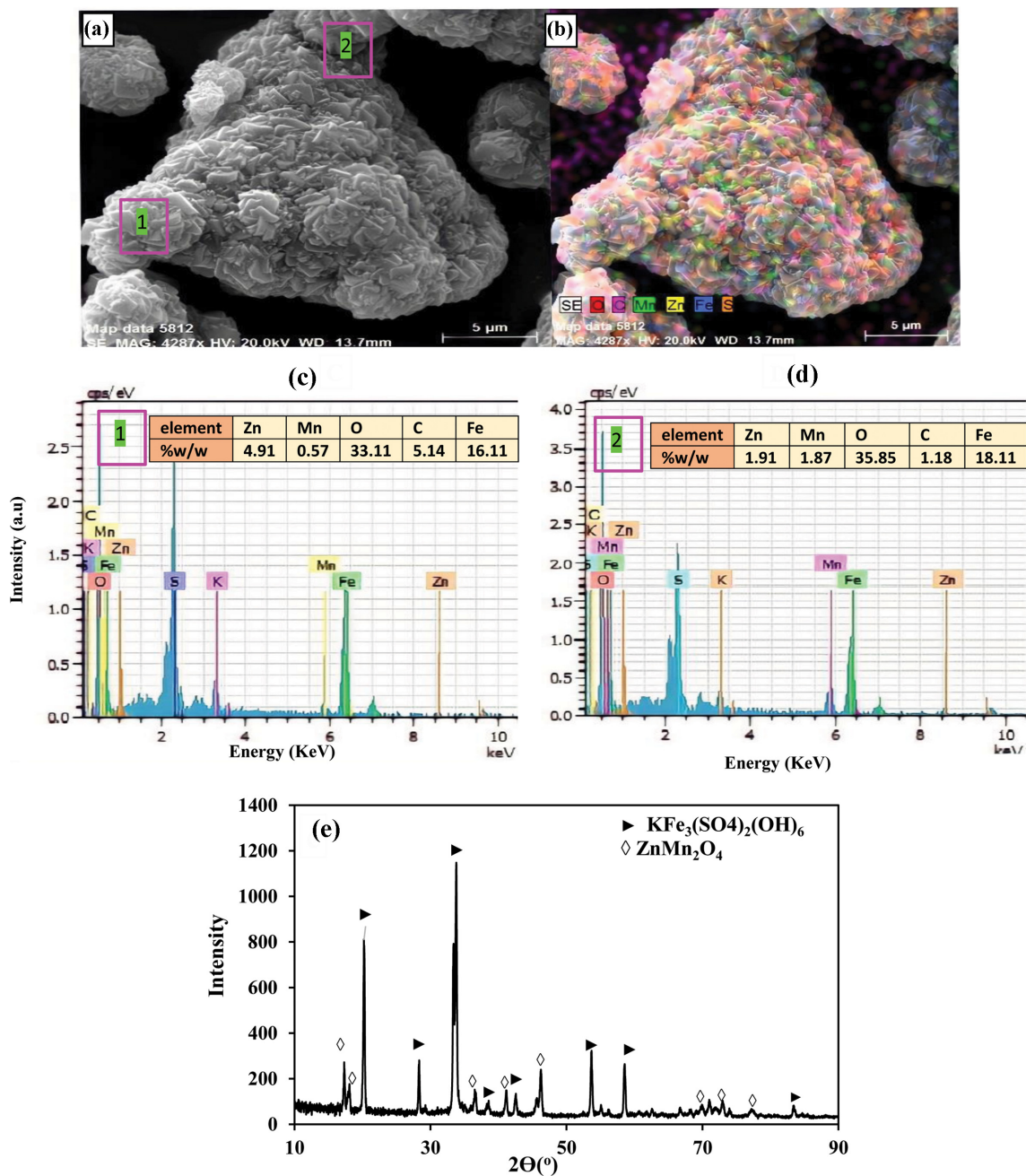


Fig. 6. (a) SEM image; (b) mapping image; (c) and (d) EDX pattern; (e) XRD pattern of bioleached BCBs-600 °C powder.

efficiencies of Zn and Mn improved to 95% and 91%, respectively, using adapted *A. ferrooxidans*. Also, this study proved that bioleaching is more efficient than chemical leaching for extraction of Zn and Mn from BCBs-600 °C powder, with 33% for Zn and 31% for Mn. It was concluded that *A. ferrooxidans* and  $\text{Fe}^{3+}$  play an important role in this process; actually, the bacteria accelerated the proton and electron transfer.

#### ACKNOWLEDGEMENTS

Part of this study was financially supported by Tarbiat Modares University under grant number IG-39701.

#### REFERENCES

1. S. Aktas, *Hydrometallurgy*, **104**, 106 (2010).
2. X. Sun, H. Hao, Z. Liu and F. Zhao, *Resour. Policy*, **65**, 101578 (2020).
3. B. Xin, W. Jiang, H. Aslam, K. Zhang, C. Liu, R. Wang and Y. Wang, *Bioresour. Technol.*, **106**, 147 (2012).
4. L. Moreno-Merino, M. E. Jiménez-Hernández, A. de la Losa and V. Huerta-Muñoz, *Sci. Total Environ.*, **526**, 187 (2015).
5. A. B. Mukherjee, R. Zevenhoven, J. Brodersen, L. D. Hylander and P. Bhattacharya, *Resour. Conserv. Recycl.*, **42**, 155 (2004).
6. S. Dev, A. Sachan, F. Dehghani, T. Ghosh, B. R. Briggs and S. Aggar-

- wal, *Chem. Eng. J.*, **397**, 124596 (2020).
7. K. Tanong, L. Coudert, G. Mercier and J. F. Blais, *J. Environ. Manage.*, **181**, 95 (2016).
  8. Y. J. Shih, S. K. Chien, S. R. Jhang and Y. C. Lin, *J. Taiwan Inst. Chem. Eng.*, **100**, 151 (2019).
  9. U. Jadhav and H. Hocheng, *J. Clean. Prod.*, **44**, 39 (2013).
  10. N. Sathaiyan, V. Nandakumar and P. Ramachandran, *J. Power Sources*, **161**, 1463 (2006).
  11. S. Leite, P. Luis, G. Carvalho, L. Rodrigues and D. Lemos, *Sep. Purif. Technol.*, **210**, 327 (2019).
  12. S. Maryam Sadeghi, G. Vanpeteghem, I. F. F. Neto and H. M. V. M. Soares, *Waste Manag.*, **60**, 697 (2017).
  13. A. Becci, A. Amato, V. Fonti, D. Karaj and F. Beolchini, *Resour. Conserv. Recycl.*, **153**, 104549 (2020).
  14. R. Sinha, G. Chauhan, A. Singh, A. Kumar and S. Acharya, *J. Environ. Chem. Eng.*, **6**, 1053 (2018).
  15. T. H. Nguyen, S. Won, M. G. Ha, D. D. Nguyen and H. Y. Kang, *Chemosphere*, **282**, 131108 (2021).
  16. M. Golzar-Ahmadi and S. M. Mousavi, *Waste Manag.*, **131**, 226 (2021).
  17. M. H. Muddanna and S. S. Baral, *J. Environ. Chem. Eng.*, **7**, 103025 (2019).
  18. H. Srichandan, R. K. Mohapatra, P. K. Parhi and S. Mishra, *Hydrometallurgy*, **189**, 105122 (2019).
  19. J. J. Roy, B. Cao and S. Madhavi, *Chemosphere*, **282**, 130944 (2021).
  20. B. K. Biswal, U. U. Jadhav, M. Madhaiyan, L. Ji, E. H. Yang and B. Cao, *ACS Sustain. Chem. Eng.*, **6**, 12343 (2018).
  21. M. S. Sadeghabad, N. Bahaloo-Horeh and S. M. Mousavi, *Hydrometallurgy*, **188**, 81 (2019).
  22. G. Belardi, R. Lavecchia, F. Medici and L. Piga, *Waste Manag.*, **32**, 1945 (2012).
  23. G. Belardi, R. Lavecchia, F. Medici, L. Piga and A. Zuorro, *Am. J. Appl. Sci.*, **11**, 1566 (2014).
  24. M. Petranikova, B. Ebin, S. Mikhailova and B. Steenari, *J. Clean. Prod.*, **170**, 1195 (2017).
  25. M. Zhang, X. Guo, B. Tian, J. Wang, S. Qi, Y. Yang and B. Xin, *Waste Manag.*, **87**, 629 (2019).
  26. T. Naseri, N. Bahaloo-Horeh and S. M. Mousavi, *J. Clean. Prod.*, **220**, 438 (2019).
  27. Z. Chen, M. Hu, B. Cui, S. Liu, D. Guo and B. Xiao, *Waste Manag.*, **48**, 383 (2016).
  28. M. Arshadi and S. M. Mousavi, *Bioresour. Technol.*, **174**, 323 (2014).
  29. C. Q. Xiao, R. A. Chi and Y. J. Fang, *Trans. Nonferrous Met. Soc. China English Ed.*, **23**, 2153 (2013).
  30. S. Ghassa, M. Noaparast, S. Ziaedin and H. Abdollahi, *Hydrometallurgy*, **171**, 362 (2017).
  31. N. J. Boxall, K. Y. Cheng, W. Bruckard and A. H. Kaksonen, *J. Hazard. Mater.*, **360**, 504 (2018).
  32. F. Pourhossein and S. M. Mousavi, *J. Hazard. Mater.*, **378**, 120648 (2019).
  33. F. Pourhossein and S. M. Mousavi, *Waste Manag.*, **79**, 98 (2018).
  34. L. Li, E. Fan, Y. Guan, X. Zhang, Q. Xue, L. Wei, F. Wu and R. Chen, *ACS Sustain. Chem. Eng.*, **5**, 5224 (2017).
  35. S. A. Charef, A. M. Affoune, A. Caballero, M. Cruz-yusta and J. Morales, *Waste Manag.*, **68**, 518 (2017).
  36. M. Petranikova, B. Ebin, S. Mikhailova, B. M. Steenari and C. Ekberg, *J. Clean. Prod.*, **170**, 1195 (2018).
  37. M. S. Song, Y. J. Cho, D. Y. Yoon, S. Nahm, S. H. Oh, K. Woo, J. M. Ko and W. I. Cho, *Electrochim. Acta*, **137**, 266 (2014).
  38. G. Belardi, F. Medici and L. Piga, *J. Power Sources*, **248**, 1290 (2014).
  39. Z. Niu, Q. Huang, J. Wang, Y. Yang, B. Xin and S. Chen, *J. Hazard. Mater.*, **298**, 170 (2015).
  40. C. A. Nogueira and F. Margarido, *Hydrometallurgy*, **157**, 13 (2015).
  41. S. Ghassa, Z. Boruomand, H. Abdollahi, M. Moradian and A. Akcil, *Sep. Purif. Technol.*, **136**, 241 (2014).
  42. M. Jjadi Bajestani, S. M. Mousavi and S. A. Shojaosadati, *Sep. Purif. Technol.*, **132**, 316 (2014).
  43. S. K. Behera and A. F. Mulaba-Bafubandi, *Korean J. Chem. Eng.*, **32**, 1447 (2015).
  44. A. Priya and S. Hait, *Process Saf. Environ. Prot.*, **143**, 262 (2020).
  45. Y. Wang, W. Zeng, G. Qiu, X. Chen and H. Zhou, *Appl. Environ. Microbiol.*, **80**, 741 (2014).
  46. A. Orell, C. A. Navarro, R. Arancibia, J. C. Mobarec and C. A. Jerez, *Biotechnol. Adv.*, **28**, 839 (2010).
  47. H. C. Jang and M. Valix, *Hydrometallurgy*, **168**, 21 (2017).
  48. Z. Niu, Q. Huang, B. Xin, C. Qi, J. Hu, S. Chen and Y. Li, *J. Chem. Technol. Biotechnol.*, **91**, 608 (2016).
  49. T. Naseri, N. Bahaloo-Horeh and S. M. Mousavi, *J. Environ. Manage.*, **235**, 357 (2019).
  50. O. Szabó and E. Farkas, *Inorg. Chim. Acta*, **376**, 500 (2011).
  51. N. V. Fomchenko and M. I. Muravyov, *Hydrometallurgy*, **174**, 116 (2017).
  52. Y. Zhang, Z. Dan, X. He, Y. Tian, J. Wang, S. Qi, N. Duan and B. Xin, *J. Clean. Prod.*, **158**, 182 (2017).
  53. Y. Xin, X. Guo, S. Chen, J. Wang, F. Wu and B. Xin, *J. Clean. Prod.*, **116**, 249 (2016).
  54. F. Ferella, I. De Michelis, F. Beolchini, V. Innocenzi and F. Vegliò, *Int. J. Chem. Eng.*, **2010**, 1 (2010).
  55. T. Naseri, N. Bahaloo-Horeh and S. M. Mousavi, *J. Environ. Manage.*, **235**, 357 (2019).
  56. B. Xin, W. Jiang, H. Aslam, K. Zhang, C. Liu, R. Wang and Y. Wang, *Bioresour. Technol.*, **106**, 147 (2012).
  57. M. Barreto, E. Jedlicki and D. S. Holmes, *Appl. Environ. Microbiol.*, **71**, 2902 (2005).
  58. H. Chu, J. Wang, B. Tian, C. Qian, T. Niu, S. Qi, Y. Yang, Y. Ge, X. Dai and B. Xin, *Chemosphere*, **275**, 130006 (2021).
  59. W. Sand and T. Gehrke, *Res. Microbiol.*, **157**, 49 (2006).
  60. J. Xiao, H. Yuan, X. Huang, J. Ma and N. Zhu, *J. Taiwan Inst. Chem. Eng.*, **96**, 453 (2019).
  61. A. H. Kaksonen, S. Särkijärvi, E. Peuraniemi, S. Junnikkala, J. A. Puhakka and O. H. Tuovinen, *Hydrometallurgy*, **168**, 135 (2017).
  62. H. Srichandan, D. J. Kim, C. S. Gahan, S. Singh and S. W. Lee, *Korean J. Chem. Eng.*, **30**, 1076 (2013).
  63. G. Belardi, R. Lavecchia, F. Medici and L. Piga, *Waste Manag.*, **32**, 1945 (2012).
  64. S. Panda, A. Akcil, S. Mishra and C. Erust, *J. Hazard. Mater.*, **325**, 59 (2017).
  65. A. Adamou, G. Manos, N. Messios, L. Georgiou, C. Xydias and C. Varotsis, *Bioresour. Technol.*, **214**, 852 (2016).